Human Flavin-Containing Monooxygenase Form 2 S-Oxygenation: Sulfenic Acid Formation from Thioureas and Oxidation of Glutathione

Marilyn C. Henderson,[†,‡] Sharon K. Krueger,[†,‡] Jan F. Stevens,[‡,§] and David E. Williams*[,†,‡]

Departments of Environmental and Molecular Toxicology and Chemistry, and The Linus Pauling Institute, Oregon State University, Corvallis, Oregon 97331

Received December 5, 2003

Thioureas are oxygenated by flavin-containing monooxygenases (FMOs), forming reactive sulfenic and/or sulfinic acids. Sulfenic acids can reversibly react with GSH and drive oxidative stress through a redox cycle. For this reason, thiourea S-oxygenation is an example of FMO-dependent bioactivation of a xenobiotic. Functional FMO2 is expressed in the lung of 26% of individuals of African descent and 5% of Hispanics but not in Caucasians or Asians. We have previously demonstrated that human FMO2.1 protein expressed in Sf9 microsomes has high activity toward a series of thioureas that are known or suspected lung toxicants including thiourea, 1-phenylthiourea, and ethylenethiourea. We now show by HPLC and LC-MS that 1-phenylthiourea and α-naphthylthiourea are converted to their sulfenic acids. GSH in the incubations at concentrations of 0.5−1.0 mM completely eliminated the sulfenic acid with resultant production of GSSG. These results indicate that individuals with the *FMO2*1* allele may be at enhanced risk of pulmonary damage upon exposure to thioureas.

Introduction

FMO[1] oxygenates numerous xenobiotics and some endobiotics containing soft nucleophiles (*1*−*3*). Five families of FMO are expressed in mammals, each with a single member (i.e., FMOs 1−5) (*4*). FMO2 is the major pulmonary FMO and is expressed at high levels in most species including nonhuman primates (*5*−*11*). A genetic polymorphism in humans is evident such that all Caucasians and Asians genotyped to date have only the *FMO2*2* allele, which codes for a truncated and nonfunctional FMO2.2A protein (*10*−*13*). The *FMO2*1* allele, which codes for full-length functional FMO2.1, is present in individuals from African (26%) and Hispanic (5%) populations (*10*−*13*). Although this genetic polymorphism has been described, the significance with respect to metabolism of FMO2 substrates in individuals carrying this allele is currently unknown.

Thiocarbamides such as TU and N,N′-mono- or disubstituted TUs are typically excellent substrates for FMO-dependent S-oxygenation (*14*−*19*). S-oxides of TUs are typically more toxic than the parent compound (*20*, *21*). The sulfenic acid product is reactive and can undergo redox cycling with GSH (*18*−*20*). Recently, Smith and Crespi demonstrated that expression of human FMO3 (but not FMO1) was toxic to mouse C3H/10T1/2 cells upon exposure to TU, PTU, or ANTU (but not ETU) and GSH appeared to protect the cells from this toxicity (*22*).

To determine if individuals expressing functional FMO2.1 protein in the lung may be at enhanced risk from TU-dependent toxicity, we assessed a series of TUs as substrates for expressed FMO2.1 by substrate-dependent NADPH oxidation (*11*). In this report, using PTU and ANTU as substrate, we determined the nature of the product. PTU and ANTU are S-oxygenated to the sulfenic acid, and co-incubation with GSH decreases the sulfenic acid.

Materials and Methods

Materials. NADPH, EDTA, potassium phosphate, FAD, PMSF, trypan blue, TU, and PTU were from Sigma (St. Louis, MO). ETU and ANTU were from Lancaster (Pelham, NH), and 1,3-DPTU was from TCI America (Portland, OR). Restriction endonucleases and T4 DNA ligase were from New England Biolabs (Beverly, MA). All of the components of the Bac-to-Bac baculovirus expression system were from Invitrogen (Carlsbad, CA). Coomassie Plus, used for protein determinations, was from Pierce (Rockford, IL).

Cloning and Expression of Human FMO2.1. A full-length cDNA clone of the *FMO2*1* allele was generated in pFastBac1 as described previously in detail (*11*). Recombinant plasmid DNA was used to transform DH10Bac competent cells, to produce recombinant bacmid, which was used to generate primary virus in Sf9 insect cells. Protein was produced in Sf9 cells from amplified tertiary or quaternary virus. FAD was supplemented (10 μg/mL) during expression. Cells were harvested 96 h postinfection, and microsomes were prepared (*9*) and resuspended in storage buffer (10 mM potassium phosphate, pH 7.6, 20% glycerol, 1 mM EDTA, and 0.4 mM PMSF). Protein concentration was determined by the method of Bradford (*23*), and flavin content was assayed by the method of Fader and Siegel (*24*). In addition to FMO2.1, full-length rabbit FMO2 cDNA was ligated into pFB1-BNE (modified pFastBac1) (*9*, *11*) and the protein was produced for comparison of kinetics with the recombinant human isoform.

* To whom correspondence should be addressed. Tel: 541-737-3277. Fax: 541-737-9766.
[†] Department of Environmental and Molecular Toxicology.
[‡] The Linus Pauling Institute.
[§] Department of Chemistry.

[1] Abbreviations: FMO, flavin-containing monooxygenase; TU, thiourea; PTU, phenylthiourea; ANTU, α-naphthylthiourea; ETU, ethylenethiourea; DPTU, diphenylthiourea; PMSF, phenylmethylsulfonylfluoride.

10.1021/tx034253s CCC: $27.50
Published on Web 04/13/2004

NADPH Oxidation. FMO-mediated substrate-dependent NADPH oxidation was performed essentially as described previously (*9*) using the various TUs as substrates. Incubation mixtures (0.5 mL) containing 100 mM Tricine/1 mM EDTA (pH 9.5), 0.1 mM NADPH, and 50 pmol/mL microsomal-expressed protein were preincubated in sample and reference cuvettes in a Cary 300 Bio UV−vis double beam spectrophotometer (Varian, Palo Alto, CA). Substrates, dissolved in water or ethanol, were added to the sample cuvette, and the change in absorbance at 340 nm was monitored for 4 min. K_m and K_{cat} were estimated from Eadie−Hofstee plots of the data generated with at least four substrate concentrations (ranging from 1 to 1000 μM) and two separate batches of expressed protein.

Incubations for HPLC and LC-MS Analysis of Metabolites. Standard microsomal incubations contained 100 mM Tricine, 1 mM EDTA (pH 9.5), and 50 μg of FMO2.1 protein in a total volume of 100 μL. Substrates were added in ethanol (not exceeding 1 μL) or water at final concentrations of 200 μM. After a 3 min incubation at 37 °C, the reactions were inititated by the addition of 1 mM NADPH and the incubation continued for 15 min. Reactions were stopped by the addition of 100 μL of methanol on ice, and the mixtures were transferred to Eppendorf tubes and centrifuged at 10 000*g* for 30 min at 4 °C. The supernatants were analyzed by HPLC and/or LC-MS. GSH was added to some incubations at concentrations ranging from 0.1 to 2 mM, either at the beginning of the incubation or after 10 min. The samples were analyzed as described.

HPLC. HPLC analysis was performed with a Waters 2690 pump equipped with a 996 diode array detector. Flow rates were 0.8 mL/min, and the column temperature was 35 °C. For PTU, the column was a Waters Nova-Pak C_{18} (4 μm, 3.9 mm × 150 mm) eluted with 20% acetonitrile and 80% 10 mM ammonium formate (pH 3.2). After 8 min at 20%, the acetonitrile was increased in a linear fashion to 35% over 3 min, held for 3 min, and returned to 20% in 3 min, and the column was equilibrated 5 min before the next injection. Detection of metabolite was monitored at 229 nm. For ANTU, samples were analyzed with an isocratic system using a Waters Polarity C_{18} (4 μm, 3.9 mm × 150 mm) column eluted with 30% acetonitrile and 70% water. Detection of metabolite was monitored at 220 nm.

Mass Spectrometry. LC-MS and LC-MS-MS analysis used a Shimadzu HPLC with LC-10 pumps connected to a Perkin-Elmer Sciex API III triple quadrupole mass spectrometer with atmospheric pressure chemical ionization (APCI) in positive ion mode with an orifice voltage of +60 V, a source temperature of 60 °C, and scanning from *m/z* 50 to 400. Samples were introduced via the heated nebulizer interface set at 450 °C. Daughter ion scanning in the MS-MS mode was used to obtain structural information with the collision energy set at 15 V. LC conditions were the same as described above for HPLC except that the temperature was ambient. Some samples containing added GSH at 200 μM were analyzed by LC-MS for GSH and GSSG. The LC flow rate was reduced to 0.1 mL/min, and the ion source was an articulated TurboIon Spray. Standard preparations of GSH and GSSG were also analyzed.

Results

TU, PTU, ETU, and ANTU (Scheme 1) were all excellent substrates for expressed human FMO2.1. The FMO2.1 enzyme expressed in Sf9 insect cell microsomes displayed typical Michaelis−Menten kinetics. The K_m and K_{cat} (or V_{max}) for S-oxygenation of each TU, as determined from substrate-dependent NADPH oxidation, is given in Table 1 and compared to previous data with human and rabbit FMO2, as well as human and pig FMO1. As is the case with rabbit FMO2 (*16*), bulky substrates with cross-sectional areas the size of DPTU (11.2 Å) are excluded from the FMO2.1 active site (*11*) and are not oxygenated (Table 1). Distinctions between orthologs can be seen in calculations of the specificity constants for rabbit and human FMO2 activity toward TUs (Table 2). For example, assayed under the same conditions, expressed rabbit and human FMO2 differ by 5-fold with respect to the specificity constant for PTU (Table 2). Kim and Ziegler (*19*) had earlier demonstrated that human FMO1 was distinct from porcine FMO1 in excluding DPTU from the active site.

HPLC analysis determined a single major polar metabolite produced following incubation of Sf9 insect cell microsomes expressing FMO2.1 with PTU (Figure 1). This peak was not present in incubations that omitted NADPH (data not shown). Subsequent analysis by LC-MS confirmed these results (Figure 2). The MS of the later eluting peak (Figure 2, top, inset) confirmed its identity as PTU (M + 1, 153) and the polar peak (Figure 2, bottom, inset) as consistent with the oxygenated (153 + 16) sulfenic acid metabolite (M + 1, 169).

Scheme 1. Chemical Structures of the TUs Examined in This Study

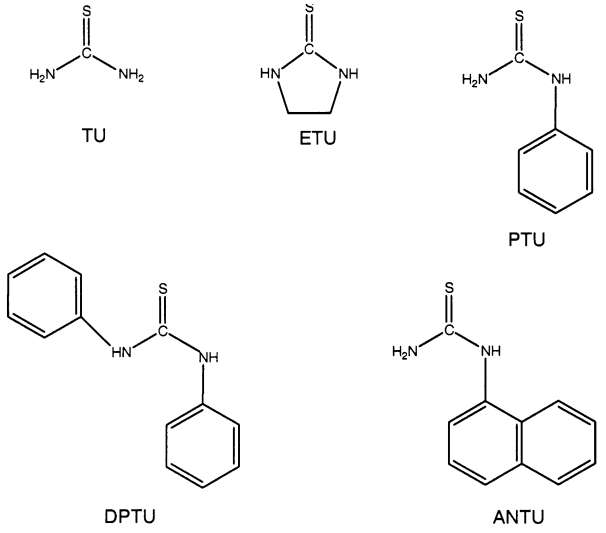

Table 1. FMO1- and FMO2-Mediated S-Oxygenation of TUs

	FMO isoform and species							
	rabbit FMO2			human FMO2		human FMO1		pig FMO1
ref	*16*[a]	*b*	*b*	*11*[b]	*11*[b]	*19*[c]	*19*[c]	*14*, *16*[a]
substrate	K_m[d]	K_m	k_{cat}[e]	K_m	k_{cat}	K_m	V_{max}	K_m
TU	23	36	134	27	51	4	21	23
ETU		21	149	14	48			34
PTU	220	82	327	29	24	3	20	4
ANTU	112	25	60	42	33			
DPTU	ND[f]	ND		ND		ND		7

[a] Assays performed at pH 7.5. V_{max} not reported. [b] Data from this manuscript. Results are mean values of two batches of Sf9 microsomes. Assays were performed at pH 9.5. [c] Assays performed at pH 7.4. [d] K_m in μM. [e] V_{max} in nmole substrate oxygenation min^{-1} mg protein^{-1} (human FMO1) or k_{cat} as min^{-1} (rabbit and human FMO2). [f] No activity was detected.

Table 2. Specificity Constants for Expressed Rabbit and Human FMO2

	rabbit FMO2	human FMO2
substrate	k_{cat}/K_m[a]	k_{cat}/K_m
TU	3.7	1.9
ETU	7.1	3.4
PTU	4.0	0.8
ANTU	2.4	0.8

[a] min^{-1} μM^{-1}

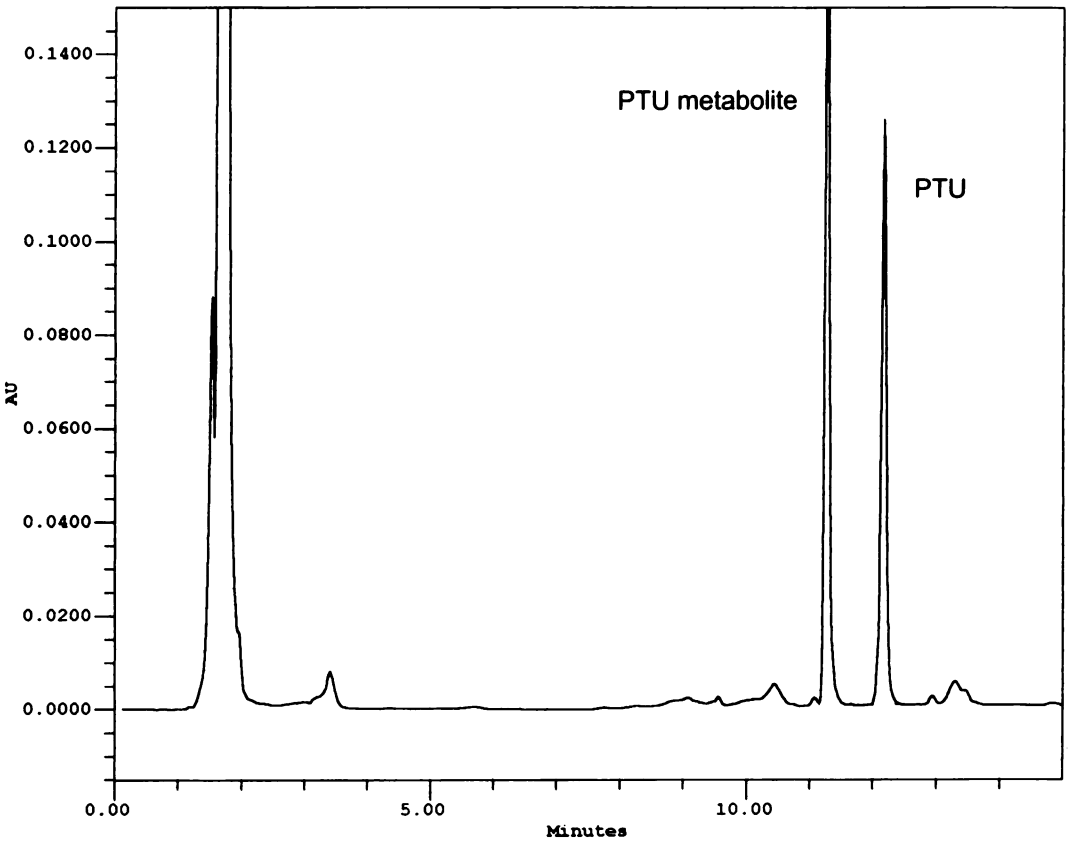

Figure 1. HPLC analysis (UV at 229 nm) of PTU and metabolites following incubation with FMO2.1.

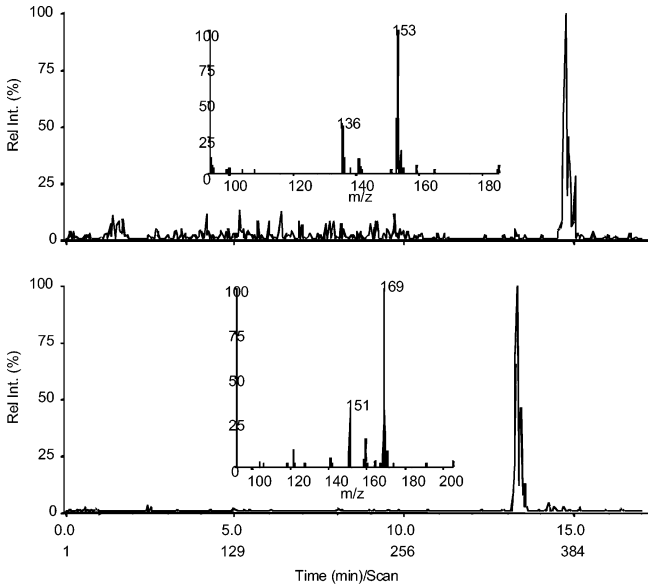

Figure 2. LC-MS of PTU incubation showing extracted ions of *m/z* 153 (PTU, top panel) and *m/z* 169 (PTU sulfenic acid, bottom panel) and corresponding mass spectra (insets).

With ANTU as the substrate, a single major polar metabolite peak was observed by HPLC analysis of the Sf9 insect microsomal incubation mixture (Figure 3). LC-MS analysis (Figure 4) showing extracted ions at *m/z* 203 (upper panel) and *m/z* 219 (bottom panel) and including the associated mass spectra (insets) confirms the identity of the latter eluting peak as the parent ANTU (M + 1, 203) and supports the identification of the polar peak eluting at 3.7 min as the ANTU sulfenic acid (M + 1, 219).

As described above, the APCI mass spectra of the sulfenic acid metabolites of PTU and ANTU showed abundant $[MH]^+$ ions whose *m/z* values (169 and 219) were consistent with the incorporation of an oxygen atom into their corresponding aryl TU substrates. To further elucidate structural possibilities, daughter ion scanning was employed. Collisional activation of these $[MH]^+$ ions produced similar MS-MS fragmentation patterns for both metabolites (PTU, Scheme 2; ANTU, Scheme 3); that is, the mass fragments of the ANTU metabolite were shifted 50 mass units (C_4H_2), which corresponds to the mass difference between ANTU and PTU (Table 3). Most fragment ions appeared to arise through loss of common oxygen, nitrogen, and sulfur species, i.e., water (18 Da), carbon monoxide (28 Da), hydrogen cyanide (27 Da), carbodiimide (HN═C═NH, 42 Da), and hydrogen sulfide (34 Da). Examination of the fragmentation patterns of the PTU and ANTU (MS spectra, Scheme 2) metabolites led us to distinguish three fragmentation pathways, of which pathway C provided direct evidence for the presence of a sulfenic acid moiety in both metabolites.

In pathway A (Scheme 2), the $[MH - H_2O]^+$ fragment loses hydrogen cyanide or carbodiimide with retention of the sulfur atom, indicating that a benzothiazole-like ring is formed upon loss of a water molecule from the $[MH]^+$ ion. The *m/z* 109 and 124 ions appear to be associated with ion peaks at *m/z* 65 and 80 because of a common mass difference of 44 Da, which can be rationalized by loss of carbon sulfide (CS) and ring contraction. A conspicuous difference between the intensities of the ion peaks that represent the $C_5H_5^+$ ion with *m/z* 65 (26% int.), originating from the PTU metabolite, and the corresponding indene fragment (*m/z* 115, 100% int.), originating from the ANTU metabolite, could be ex-

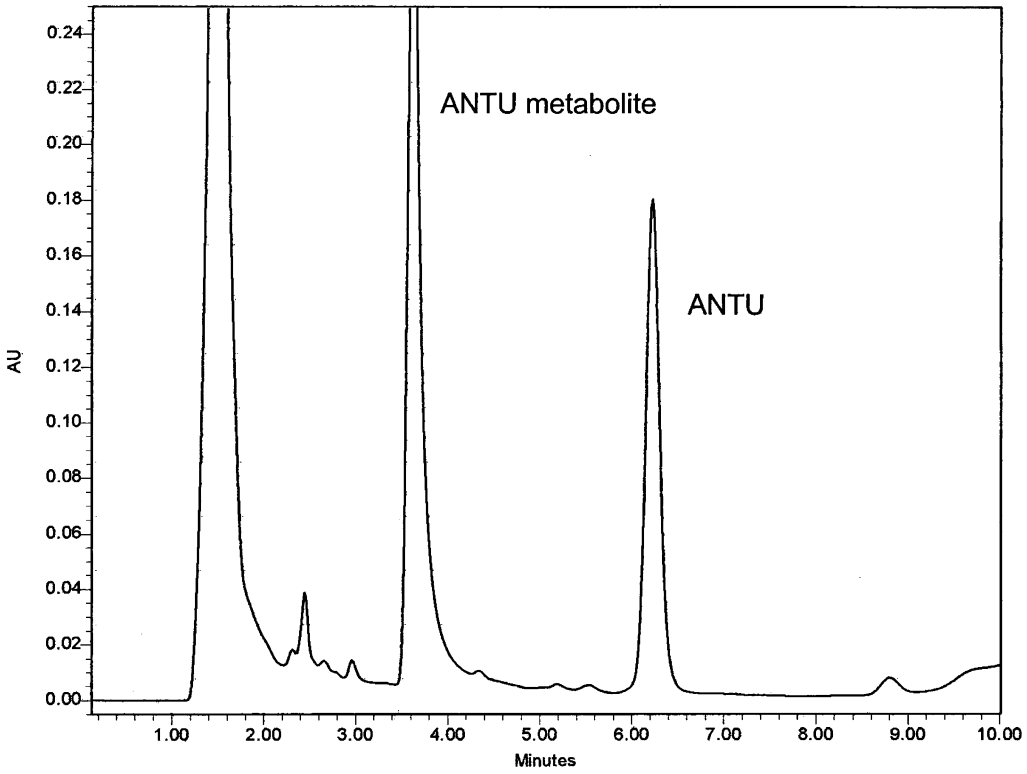

Figure 3. HPLC analysis (UV at 220 nm) of ANTU and metabolites following incubation with FMO2.1.

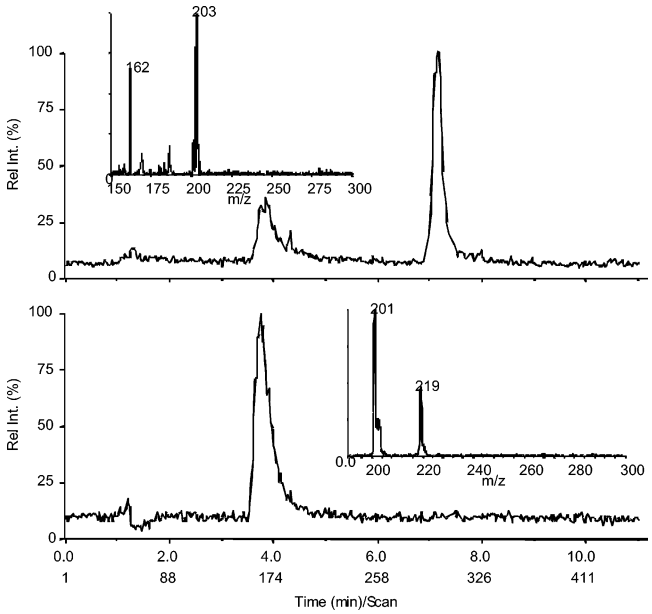

Figure 4. LC-MS of ANTU incubation showing extracted ions of *m/z* 203 (ANTU, top panel) and *m/z* 219 (ANTU sulfenic acid, bottom panel) and corresponding mass spectra (insets).

plained by stabilization through extended delocalization of the positive charge in the indene nucleus (Scheme 3).

Pathway B (Scheme 2) is characterized by a fragment ion, *m/z* 135 $[MH - H_2S]^+$, that must contain the oxygen atom from the sulfenic acid moiety because there is no other way to account for a mass difference of 34 Da. The loss of a sulfur species with retention of oxygen suggests a rearrangement reaction as shown in Scheme 2, which is supported by subsequent loss of carbon monoxide, a common fragmentation reaction in quinones and quinonimines, and hydrogen cyanide. The resulting fragment is the immonium ion with *m/z* 80, and at this point, pathways A and B seem to converge.

Pathway C (Scheme 2) is characterized by initial loss of the sulfenic acid moiety, giving rise to a fragment ion with *m/z* 119 $[MH - H_2SO]^+$ in the case of the PTU metabolite. Although pathways A and B produce fragments that are consistent with the structure of the sulfenic acid metabolites, the loss of a neutral H_2SO species can be taken as evidence for the presence of a sulfenic acid moiety in both metabolites. Subsequent loss of hydrogen cyanide and carbodiimide from the *m/z* 119 ion yields an azepine-like fragment (*m/z* 92) and a fragment with *m/z* 77 that is often observed in mass spectra of substituted benzenes. In the MS-MS spectrum of the ANTU metabolite, pathway C appears to be directed toward the formation of the azepine-like fragment (*m/z* 142) from the initial fragment with *m/z* 169 $[MH - H_2SO]^+$.

Addition of increasing amounts of GSH to incubations containing PTU or ANTU to Sf9 insect cell microsomes containing FMO2.1 resulted in a concentration-dependent reduction in the yield of the PTU or ANTU sulfenic acid metabolites (Figure 5). Concentrations of GSH as low as 0.5 mM completely eliminated the PTU sulfenic acid and decreased the ANTU sulfenic acid by 93.5%. This effect was apparent even when the GSH was added 10 min into the 15 min incubation period. Incubations containing equimolar amounts of added GSH and PTU or ANTU were further analyzed by LC-MS as described. GSSG/GSH ratios were calculated from total ion current values for the extracted ions (GSSG, *m/z* 613; GSH, *m/z* 308) for each individual sample run. Although not an absolute value, the ratio reflects the proportion of GSH converted to GSSG in each analysis and gives a basis for comparison. Results are shown in Figure 6 and indicate

Scheme 2. MS-MS Fragmentation Scheme of Arylthiourea Sulfenic Acid Metabolites with MS-MS of PTU Sulfenic Acid (See Also Table 2)

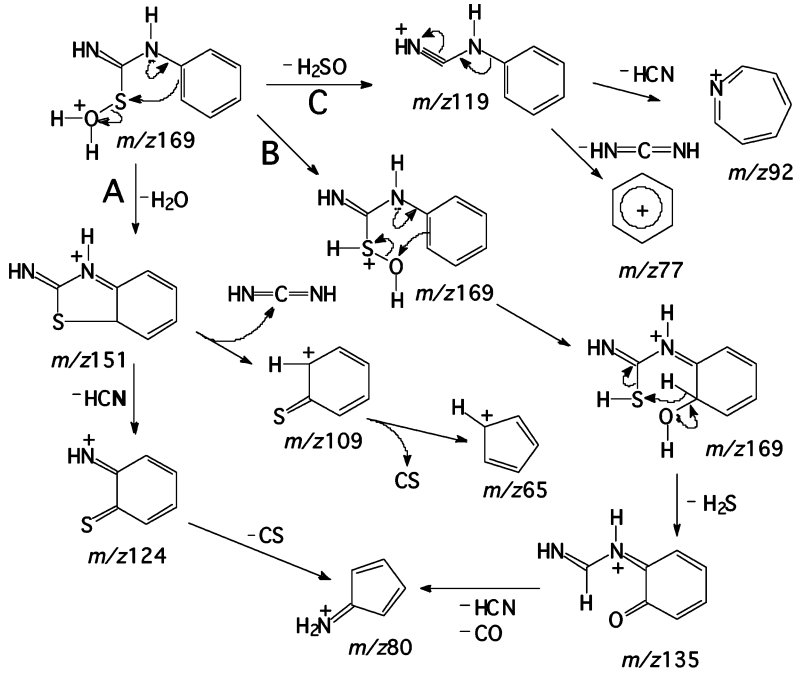

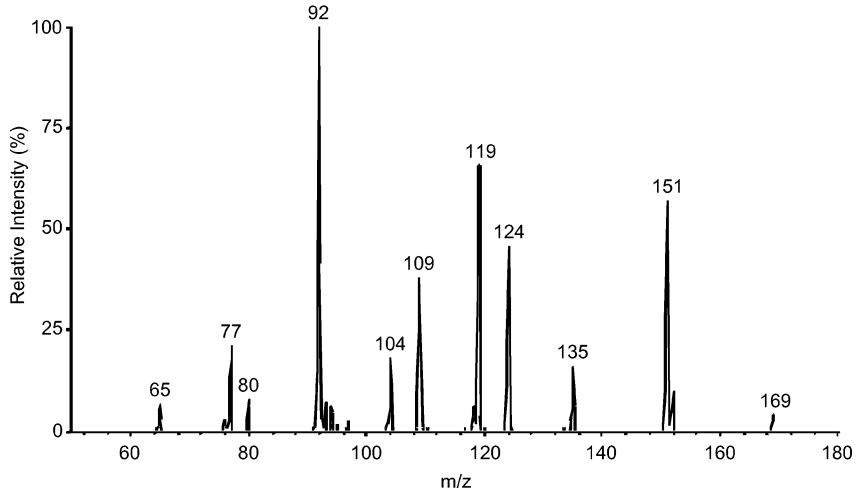

Scheme 3. MS-MS of ANTU Sulfenic Acid (See Also Table 2) and Formation of Ions *m/z* 159 and *m/z* 115 via Pathway A: Resonance Stabilization of the Indene Carbocation

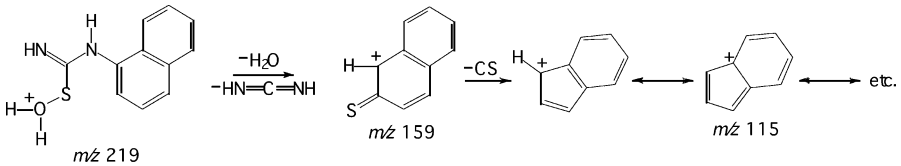

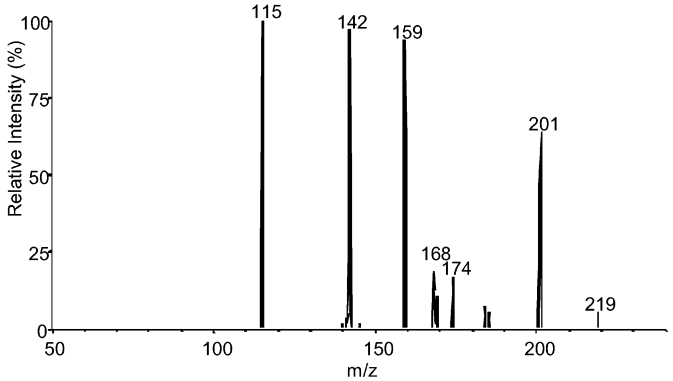

Table 3. MS-MS Fragmentation Behavior of the Sulfenic Acid Metabolites of Arylthioureas

fragmentation pathway (Scheme 2)	fragment species	observed *m/z* (int. %) PTU, sulfenic acid metabolite	observed *m/z* (int. %) ANTU, sulfenic acid metabolite
A	$[MH]^+$	*m/z* 169 (5)	*m/z* 219 (6)
	$[MH - H_2O]^+$	*m/z* 151 (57)	*m/z* 201 (65)
	$[MH - H_2O - HCN]^+$	*m/z* 124 (46)	*m/z* 174 (17)
	$[MH - H_2O - HNCNH]^+$	*m/z* 109 (38)	*m/z* 159 (94)
	$[MH - H_2O - HNCNH - CS]^+$	*m/z* 65 (6)	*m/z* 115 (100)
B	$[MH - H_2S]^+$	*m/z* 135 (16)	*m/z* 185 (5)
	$[MH - H_2S - HCN - CO]^+$	*m/z* 80 (8)	*m/z* 130 (−)
C	$[MH - H_2SO]^+$	*m/z* 119 (66)	*m/z* 169 (11)
	$[MH - H_2SO - HNCNH]^+$	*m/z* 77 (21)	*m/z* 127 (−)
	$[MH - H_2SO - HCN]^+$	*m/z* 92 (100)	*m/z* 142 (97)

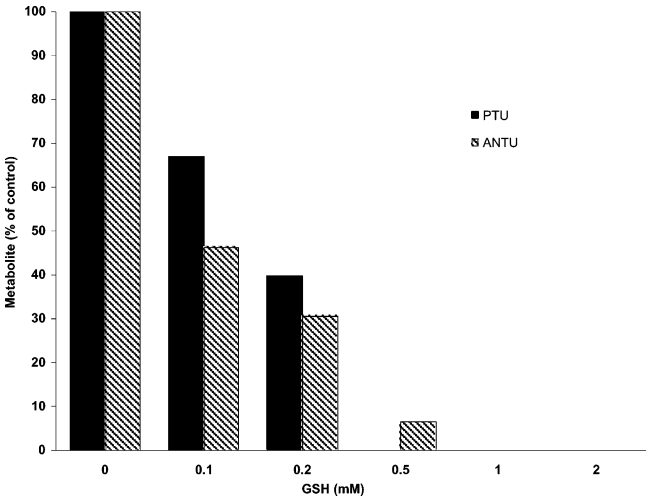

Figure 5. Effect of GSH addition to the incubation on the yield of PTU and ANTU sulfenic acids.

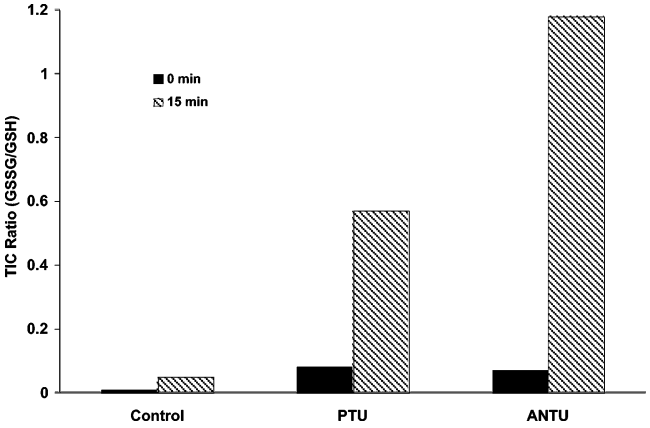

Figure 6. Conversion of GSH to GSSG in microsomal incubations containing PTU and ANTU. The TIC ratio is the ratio of the total ion current of the extracted ions at 613 and 308. Controls were incubations containing either no substrate or no NADPH (similar result not shown).

a large increase in the amount of GSSG present in the incubations producing the sulfenic acid metabolites. This supports the redox cycling effect of the PTU sulfenic acid depicted in Scheme 4.

Discussion

The major FMO in pulmonary microsomes of most mammals, including nonhuman primates, is FMO2. FMO2 is expressed at relatively high levels in pulmonary microsomes, accounting for 5−10% of the total protein in some species such as the rabbit (*6*). Humans are an exception, and FMO2 is expressed in an ethnically dependent genetic polymorphic fashion (*10*−*13*). All Caucasians and Asians genotyped to date have the *FMO2*2* allele in which a C→T transition at bp1414 replaces a gln at amino acid residue 472 with a premature stop codon (*10*). The truncated FMO2.2A protein is catalytically nonfunctional and is not detectable in human lung microsomes (*10*−*13*), probably due to improper folding and rapid degradation. Twenty-six percent of individuals of African descent and about 5% of Hispanics have at least one *FMO2*1* allele (*10*−*13*). The product of the *FMO2*1* allele, FMO2.1, is 97% identical to the Rhesus FMO2 and 85% identical to the rabbit and mouse FMO2. On the basis of a single individual, genotyped as *FMO2*1*/*FMO2*2*, we estimated the specific content of FMO2.1 in lung microsomes at 8.8 pmol/mg, which is comparable, if not higher than, most cytochromes P450 (CYPs) expressed in human lung. The rat is interesting in that domestic strains (Sprague−Dawley and Wistar) resemble humans in having a truncated FMO2, whereas the wild rat (*Rattus rattus*) expresses the full-length functional FMO2 (*25*).

TU is an industrial chemical with a number of uses that is produced in large amounts in the U.S. (over 10 000 tons per year). TU is an antithyroid agent and carcinogen in rodents apparently as a result of S-oxygenation (*26*). TU is an excellent substrate for FMO, and S-oxygenation leads to formation of the sulfenic acid (*14*−*19*). The sulfenic acid in turn can be further oxidized to the sulfinic acid or combine with GSH (Scheme 4) (*18*−*20*) with the net result being conversion of GSH to oxidized GSH (GSSG) and regeneration of TU. In the presence of GSH reductase, a redox cycle is established, which can lead to oxidative stress and toxicity (*27*, *28*). In addition to GSH, the sulfenic acid metabolite of TUs can react with other sulfhydryls including cysteine residues in various proteins. FMO-mediated S-oxygenation of TUs leads to covalent binding to proteins (*29*). By this mechanism, FMO-dependent oxygenation of PTU was shown to inhibit CYP1A1 and activate GSH S-transferase in rat liver microsomes (*30*). Alteration in the function of cellular proteins through modification of critical cysteine sulfhydryls may be an important mechanism for toxicity of TUs. The FMO protein itself does not appear to be a target for the reactive metabolites generated, and no evidence for an FMO mechanism-based (suicide substrate) inhibitor exists.

TU, PTU, ETU, and ANTU (but not DPTU) were found to be excellent substrates for human FMO2.1 with K_{ms} in the low micromolar range. HPLC and LC-MS analysis, following incubation with PTU or ANTU, showed the major metabolite to be the sulfenic acid, the appearance

Scheme 4. Diagram Depicting the FMO-Dependent Redox Cycling of PTU in the Presence of GSH (Adapted from Ref *22*)

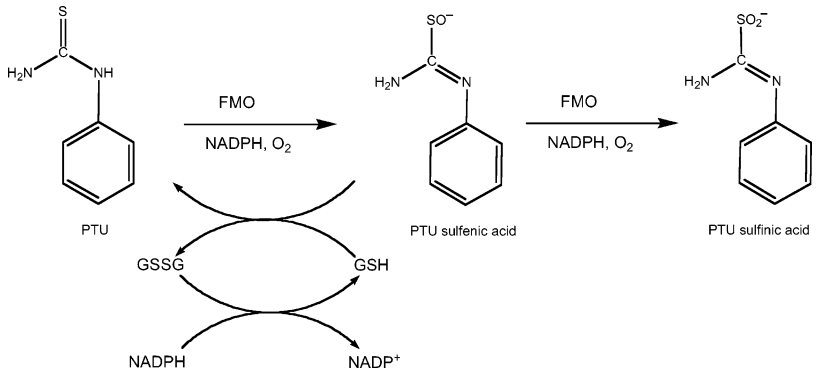

of which was completely eliminated at concentrations of 0.5 mM GSH or higher.

ANTU is toxic to the lung via production of severe pulmonary edema and vascular injury, which, again, appears to be dependent upon S-oxygenation, covalent binding to proteins, and GSH depletion (*31*−*35*). ANTU is an excellent substrate for FMOs including lung FMO2. ANTU displays an interesting species selectivity, which is one of the reasons for its use as a rodenticide. As domestic strains of rat express the nonfunctional truncated protein, we would predict that wild rats would be more susceptible to FMO2-mediated pulmonary toxicity following exposure to ANTU. It would be of interest to determine if species differences in sensitivity correlate to FMO2 activity toward ANTU. We observed one major metabolite by HPLC following incubation of ANTU with Sf9 insect cell microsomes expressing FMO2.1. The major metabolite was identified as the sulfenic acid based upon LC-MS and MS-MS. As with PTU, addition of GSH to the incubation mixture completely eliminated the sulfenic acid metabolite. The fact that the metabolite disappears even when the GSH is added after 10 min of incubation suggests that the disappearance is due to reaction with GSH rather than the GSH causing an inhibition of the enzyme or some other reaction component.

ETU is a breakdown product of numerous fungicides (zineb, nabam, mancozeb, and metiram) and is a carcinogen, teratogen, and pulmonary toxicant (*36*−*40*). The metabolism of ETU is more complicated than that of TU, PTU, or ANTU, as products other than the sulfenic and sulfinic acids are observed (*17*, *41*). The FMO has been shown to play a major role in the S-oxygenation of ETU and production of covalent adducts with proteins (*17*). In this manuscript, we show ETU to be an excellent substrate for human FMO2.1 with the lowest K_m (14 μM) and the highest specificity constant (3.4 min^{-1} μM) of any of the TUs examined. We were not successful in identification of the FMO2-oxygenated metabolite(s) of ETU, perhaps due to a greater reactivity of the sulfenic acid leading to rapid loss through covalent adduction to protein or other nucleophilic targets in the microsomal incubations.

In conclusion, we have shown that human FMO2.1, expressed in certain ethnic groups, is very effective at S-oxygenation of TUs, an important class of industrial chemicals and pesticides and a minor class of therapeutics. The major metabolite is the sulfenic acid, which binds sulfhydryl groups such as GSH or protein cysteine residues. The redox cycling of the sulfenic acid with GSH can induce oxidative stress, which may be a mechanism of toxicity as could the modification of critical cysteine residues in proteins with important cellular functions. Although FMOs are capable of carrying out the second oxygenation to the sulfinic acid, the K_m is typically much higher (*14*). With PTU or ANTU as substrate, we found no evidence for production of the sulfinic acid. The major conclusion with respect to human health is that based on our findings, we predict that individuals with the *FMO2*1* allele would be at greater risk for development of pulmonary toxicity following exposure to TUs. S-Oxygenation of TUs can also be catalyzed by CYPs, but FMO-mediated metabolism appears to predominate (*30*), especially in extrahepatic tissues where the ratio of FMO/CYP is higher. It would be of interest to determine the relative contribution of CYP to FMO in the S-oxygenation of TUs utilizing pulmonary microsomes of individuals lacking or expressing the *FMO2*1* allele.

Acknowledgment. This study was supported by PHS Grant HL38650. We also acknowledge support from the Cell Culture Facility Core and Jeff Morré of the Mass Spectrometry Facility Core of the Oregon State University Environmental Health Sciences Center (ES 00210). We also acknowledge the laboratory assistance provided by Lisbeth Siddens, Isaac Emery, and Jonathan Van Dyke.

References

(1) Ziegler, D. M. (1993) Recent studies on the structure and function of multisubstrate flavin-containing monooxygenases. *Annu. Rev. Pharmacol. Toxicol. 33*, 179−199.

(2) Cashman, J. R. (1995) Structural and catalytic properties of the mammalian flavin-containing monooxygenase. *Chem. Res. Toxicol. 8*, 165−181.

(3) Ziegler, D. M. (2003) An overview of the mechanism, substrate specificities, and structure of FMOs. *Drug Metab. Rev. 34*, 503−511.

(4) Lawton, M., Cashman, J., Cresteil, T., Dolphin, C., Elfarra, A., Hines, R. N., Hodgson, E., Kimura, T., Ozols, J., Phillips, I., Philpot, R., Poulsen, L., Rettie, S., Williams, D., and Ziegler, D. (1994) A nomenclature for the mammalian flavin-containing monooxygenase gene family based on amino acid sequence identities. *Arch. Biochem. Biophys. 308*, 254−257.

(5) Wyatt, M. K., Philpot, R. M., Carver, G., Lawton, M. P., and Nikbakht, K. N. (1996) Structural characteristics of flavin-containing monooxygenase genes one and two (*FMO1* and *FMO2*). *Drug Metab. Dispos. 24*, 1320−1327.

(6) Williams, D. E., Hale, S. E., Muerhoff, A. S., and Masters, B. S. S. (1985) Rabbit lung flavin-containing monooxygenase. Purification, characterization and induction during pregnancy. *Mol. Pharmacol. 28*, 381−390.

(7) Tynes, R. E., Sabourin, P. J., and Hodgson, E. (1985) Identification of distinct hepatic and pulmonary forms of microsomal flavin-containing monooxygenase in the mouse and rabbit. *Biochem. Biophys. Res. Commun. 126*, 1069−1075.

(8) Karoly, E. D., and Rose, R. L. (2001) Sequencing, expression, and characterization of cDNA expressed flavin-containing monooxygenase 2 from mouse. *J. Biochem. Mol. Toxicol. 15*, 300−308.
(9) Krueger, S. K., Yueh, M.-F., Martin, S. R., Pereira, C. B., and Williams, D. E. (2001) Characterization of expressed full-length and truncated FMO2 from rhesus monkey. *Drug Metab. Dispos. 29*, 693−700.
(10) Dolphin, C. T., Beckett, D. J., Janmohamed, A., Cullingford, T. E., Smith, R. L., Shepard, E. A., and Philpot, R. M. (2001) The flavin-containing monooxygenase 2 gene (FMO2) of humans, but not of other primates, encodes a truncated, nonfunctional protein. *J. Biol. Chem. 273*, 30599−30607.
(11) Krueger, S. K., Martin, S. R., Yueh, M.-F., Pereira, C. B., and Williams, D. E. (2001) Identification of active flavin-containing monooxygenase isoform 2 in human lung and characterization of expressed protein. *Drug Metab. Dispos. 30*, 34−41.
(12) Whestine, J. R., Yueh, M.-F., Hopp, K. A., McCarver, D. G., Williams, D. E., Park, C.-S., Kang, J. H., Cha, Y.-N., Dolphin, C. T., Shephard, E. A., Phillips, I. R., and Hines, R. N. (2000) Ethnic differences in human flavin-containing monooxygenase 2 (*FMO2*) polymorphisms: detection of expressed protein in African Americans. *Toxicol. Appl. Pharmacol. 168*, 216−224.
(13) Krueger, S. K., Williams, D. E., Yueh, M.-F., Martin, S. R., Hines, R. N., Raucy, J. L., Dolphin, C. T., Shephard, E. A., and Phillips, I. R. (2002) Genetic polymorphisms of flavin-containing monooxygenase (FMO) *Drug Metab. Rev. 34*, 523−532.
(14) Poulsen, L. L., Hyslop, R. M., and Ziegler, D. M. (1979) S-Oxygenation of N-substituted thioureas catalyzed by the pig liver microsomal FAD-containing monooxygenase. *Arch. Biochem. Biophys. 198*, 78−88.
(15) Sabourin, P. J., and Hodgson, E. (1984) Characterization of the purified microsomal FAD-containing monooxygenase from mouse and pig liver. *Chem-Biol. Interact. 51*, 125−139.
(16) Nagata, T., Williams, D. E., and Ziegler, D. M. (1990) Substrate specificities of rabbit lung and porcine liver flavin-containing monooxygenases: differences due to substrate size. *Chem. Res. Toxicol. 3*, 372−376.
(17) Decker, C. J., and Doerge, D. R. (1991) Rat hepatic microsomal metabolism of ethylenethiourea. Contributions of the flavin-containing monooxygenase and cytochrome P-450 isozymes. *Chem. Res. Toxicol. 4*, 482−489.
(18) Guo, W. X., Poulsen, L. L., and Ziegler, D. M. (1992) Use of thiocarbamides as selective substrate probes for isoforms of flavin-containing monooxygenases. *Biochem. Pharmacol. 44*, 2029−2037.
(19) Kim, Y. M., and Ziegler, D. M. (2000) Size limits of thiocarbamides accepted as substrates by human flavin-containing monooxygenase 1. *Drug Metab. Dispos. 28*, 1003−1006.
(20) Ziegler, D. M. (1982) Functional groups bearing sulfur. In *Metabolism of Functional Groups* (Jakoby, W. B., Bend, J. R., Caldwell, J., Eds.) pp 171−184, Academic Press, New York.
(21) Neal, R. A., and Halpert, J. (1982) Toxicology of thiono-sulfur compounds. *Annu. Rev. Pharmacol. Toxicol. 22*, 321−339.
(22) Smith, P. B., and Crespi, C. (2002) Thiourea toxicity in mouse C3H/10T1/2 cells expressing human flavin-dependent monooxygenase 3. *Biochem. Pharmacol. 63*, 1941−1948.
(23) Bradford, M. M. (1976) A rapid and sensitive method for the quantitation of microgram quantities of protein utilizing the principle of protein-dye binding. *Anal. Biochem. 72*, 248−254.
(24) Fader, E. J., and Siegel, L. M. (1973) A raid micromethod for determination of FMN and FAD in mixtures. *Anal. Biochem. 53*, 332−336.
(25) Lattard, V., Longin-Sauvageon, C., Krueger, S. K., Williams, D. E., and Benoit, E. (2002) The FMO2 gene of laboratory rats, as in most humans, encodes a truncated protein. *Biochem. Biophys. Res. Commun. 292*, 558−563.
(26) Ziegler-Skylakakis, K., Nill, S., Pan, J.-F., and Andrae, U. (1998) S-Oxygenation of thiourea results in the formation of genotoxic products. *Environ. Mol. Mutagen. 31*, 362−373.
(27) Krieter, P. A., Ziegler, D. M., Hill, K. E., and Burk, R. F. (1984) Increased biliary GSSG efflux from rat livers perfused with thiocarbamide substrates for the flavin-containing monooxygenase. *Mol. Pharmacol. 26*, 122−127.
(28) Onderwater, R. C., Commandeur, J. N., Groot, E. J., Sitters, A., Menge, W. M., and Vermeulen, N. P. (1998) Cytotoxicity of a series of mono- and di-substituted thioureas in freshly isolated rat hepatocytes: a preliminary structure-toxicity relationship study. *Toxicology 125*, 117−129.
(29) Decker, C. J., and Doerge, D. R. (1992) Covalent binding of ^{14}C- and ^{35}S-labeled thiocarbamides in rat hepatic microsomes. *Biochem. Pharmacol. 43*, 881−888.
(30) Onderwater, R. C. A., Commandeur, J. N. M., Menge, W. M. P. B., and Vermeulen, N. P. E. (1999) Activation of microsomal glutathione S-transferase and inhibition of cytochrome P450 1A1 activity as a model system for detecting protein alkylation by thiourea-containing compounds in rat liver microsomes. *Chem. Res. Toxicol. 12*, 396−402.
(31) Scott, A. M., Powell, G. M., Upshall, D. G., and Curtis, C. G. (1990) Pulmonary toxicity of thioureas in the rat. *Environ. Health Perspect. 85*, 43−50.
(32) Boyd, M. R., and Neal, R. A. (1976) Studies on the mechanism of toxicity and of development of tolerance to the pulmonary toxin, alpha-naphthylthiourea (ANTU). *Drug Metab. Dispos. 4*, 314−322.
(33) Lee, P. W., Arnau, T., and Neal, R. A. (1980) Metabolism of alpha-naphthylthiourea by rat liver and rat lung microsomes. *Toxicol. Appl. Pharmacol. 53*, 164−173.
(34) Hardwick, S. J., Skamarauskas, J. T., Smith, L. L., Upshall, D. G., and Cohen, G. M. (1991) Protection of rats against the effects of alpha-naphthylthiourea (ANTU) by elevation of nonprotein sulphydryl levels. *Biochem. Pharmacol. 42*, 1203−1208.
(35) Barton, C. C., Bucci, T. J., Lomax, L. G., Warbritton, A. G., and Mehendale, H. M. (2000) Stimulated pulmonary cell hyperplasia underlies resistance to α-naphthylthiourea. *Toxicology 143*, 167−181.
(36) Houeto, P., Bindoula, G., and Hoffman, J. R. (1995) Ethylenebisdithiocarbamates and ethylenethiourea: possible human health hazards. *Environ. Health Perspect. 103*, 568−573.
(37) Vettorazzi, G., Almeida, W. F., Burin, G. J., Jaeger, R. B., Puga, F. R., Rahde, A. F., Reyes, F. G., and Schvartsman, S. (1995−96) International safety assessment of pesticides: dithiocarbamate pesticides, ETU, and PTU—a review and update. *Teratog., Carcinog., Mutagen. 15*, 313−317.
(38) National Toxicology Program. (1992) NTP toxicology and carcinogenesis studies of ethylene thiourea (CAS: 96-45-7) in F344 rats and B6C3F1 mice (feed studies). *Natl. Toxicol. Prog. Tech. Rep. Ser. 388*, 1−256.
(39) Chhabra, R. S., Eustis, S., Haseman, J. K., Kurtz, P. J., and Carlton, B. D. (1992) Comparative carcinogenicity of ethylene thiourea with or without perinatal exposure in rats and mice. *Fundam. Appl. Toxicol. 18*, 405−417.
(40) Saillenfait, A. M., Sabate, J. P., Langonne, I., and DeCeaurriz, J. (1991) Difference in the developmental toxicity of ethylenethiourea and three N,N′-substituted thiourea derivatives in rats. *Fundam. Appl. Toxicol. 17*, 399−408.
(41) James, J. P., Quistad, G. B., and Casida, J. E. (1995) Ethylenethiourea S-oxidation products: preparation, degradation, and reaction with proteins. *J. Agric. Food Chem. 43*, 2530−2535.

TX034253S